IINS, FT-IR and DFT Study of the Internal Dynamics of [4-apyH][SbCl$_4$]

K. Hołderna-Natkaniec[a,b,*], I. Natkaniec[c,b], E. Mikuli[d],
J. Swiergiel[a], V.D. Khavryutchenko[e] and R. Jakubas[f]

[a]Institute of Physics, A. Mickiewicz University
Umultowska 85, 61-614 Poznań, Poland
[b]Frank Laboratory of Neutron Physics, JINR, Dubna 141980, Russia
[c]H. Niewodniczański Institute of Nuclear Physics, PAS
Radzikowskiego 152, 31-342 Kraków, Poland
[d]Department of Chemical Physics, Jagiellonian University
Ingardena 3, 30-060 Kraków, Poland
[e]Institute of Surface Chemistry, Ukrainian Academy of Science
Kiev, Ukraine
[f]Faculty of Chemistry, University of Wrocław
Joliot-Curie 14, 50-383 Wrocław, Poland

Dedicated to Professor Jerzy Janik on the occasion of his 80th birthday

A combination of infrared and inelastic incoherent neutron scattering spectroscopies with the density functional theory and semi-empirical calculations was applied to propose an assignment of the vibrational spectra of 4-aminopyridine chloroantimonate(IV).

PACS numbers: 78.70.Nx, 33.20.Ea, 77.84.–s, 31.15.E–

1. Introduction

The subject of our investigation is an ionic-molecular crystal built of the organic 4-aminopyridine cation [4-apyH]$^+$ and the inorganic anion [SbCl$_4$]$^-$. The crystal undergoes a few phase transitions at 240/240.5, 248.5/250, 270.5/271, 304/304 K, respectively, on the cooling/heating runs. The symmetries of the monoclinic elementary cell in the subsequent phases numbered from V to I on heating are as follows: $P2_1/c \leftrightarrow (Cc) \leftrightarrow Cc \leftrightarrow C2/c \leftrightarrow C2/c$ [1]. The crystal of

*corresponding author; e-mail: natkanie@amu.edu.pl

[4-$NH_2C_5H_4NH$][$SbCl_4$] (abbreviation [4-apyH][$SbCl_4$]) shows ferroelectric properties in the temperature range from 240.5 to 271 K. The crystalline structure is built of sheets of planar cations [4-apyH]$^+$ separated by the chain of tetrahedral anions [$SbCl_4$]$^-$. The [4-apyH]$^+$ cation is surrounded by a few anions and some close contact interactions of the hydrogen bridge type can be distinguished [2–8]. Although the hydrogen atoms of NH_2, CH, and NH^+ groups were in close contact with the anion, the strongest hydrogen bridge bond is formed between the imide (NH^+) group and the anion. The strongest interaction is modelled in our study.

The molecular dynamics of the crystal was studied by the neutron and the infrared (IR) spectroscopies. The neutron vibrational spectra give the frequencies and intensities of all normal modes; their intensities were proportional to the displacement of each atom performing the vibrations and the incoherent cross-section for scattered nucleus (value of incoherent cross-section of proton is several times greater than that of nitrogen or carbon atoms, building the cation studied [9]). The IR intensity is proportional to the changes in the electrical dipole moment of the molecule.

To make the assignment of the subsequent bands in the spectra, the structure of the simple complex was optimised and the frequencies and intensities of the normal modes were calculated by the density functional theory (DFT) [10] and semi-empirical PM3 [11] methods. The interaction N1–H$^+$...Cl is the short-
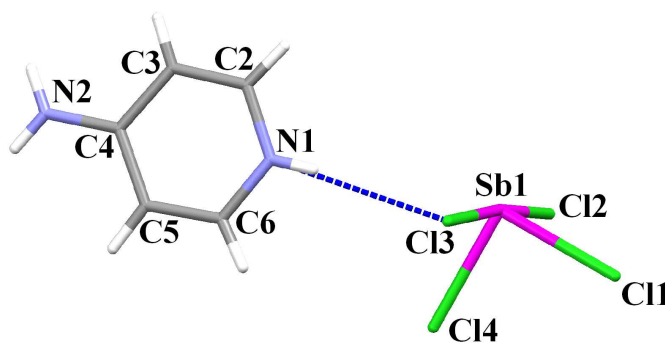

Fig. 1.   Structure of the isolated molecule of [4-apyH][$SbCl_4$] with the atom numbering scheme [2–8].

est one, according to crystallographic data [2]. Therefore, the optimisation of the complex structure was performed, where this bridge is responsible for the interaction between the cation and the anion. The structure of the complex with the atom numbering system is presented in Fig. 1.

2. Method

The inelastic incoherent neutron scattering (IINS) spectra of the crystal studied were recorded as a function of the incident neutrons wavelength at different temperatures on a NERA-PR spectrometer in Dubna, co-working with a pulse

reactor IBR-2 [12]. The Fourier transform infrared (FT-IR) absorption measurements were performed on a Bruker-EQUINOX 55 Fourier transformed infrared spectrometer.

The quantum mechanical calculation of the frequency and intensity of normal modes were performed by semi-empirical method as less time consuming, and by the density functional theory method using Gaussian 03 package [13].

3. Results and discussion

The IINS spectra of the crystal studied were recorded as a function of the wavelength of the incident neutrons at 20, 240, 260, and 290 K. The IINS spectra were converted into the phonon density of states spectra $G_{\mathrm{exp}}(\nu)$ as shown in Fig. 2.
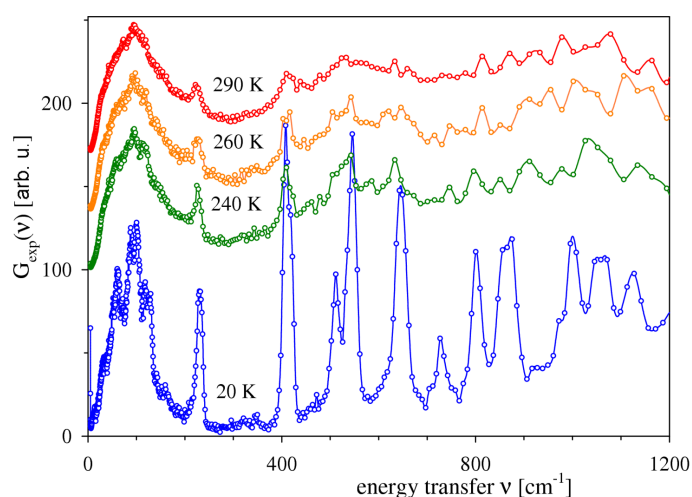

Fig. 2. Phonon density of state spectra of [4-apyH][SbCl$_4$] obtained at different temperatures after transformation of the IINS spectra in one phonon scattering approximation, $G_{\mathrm{exp}}(\nu)$.

The low temperature $G_{\mathrm{exp}}(\nu)$ spectra show a well separated band above the energy gap of 240–350 cm^{-1}, but below 700 cm^{-1}. Its band width is close to the resolution power of the spectrometer. When the energy transfer increased, the intensity of selected bands as well as resolution power decreased [14, 9] according to the scattering law. In the low temperature $G_{\mathrm{exp}}(\nu)$ spectra one may distinguish well separated bands at 230.4, 407.8, 510.0, 544.8, 800.5 cm^{-1}. Although on heating the intensity of the bands decreased, at room temperature the lattice branch and internal normal vibrational modes can be separated.

The FT-IR spectrum measured at 20 K (in nujol) is shown in the wave number range from 450 to 3500 cm^{-1} in Fig. 3. As in the range from 1750 to 2580 cm^{-1} no bands were observed, this part of the spectrum was neglected.
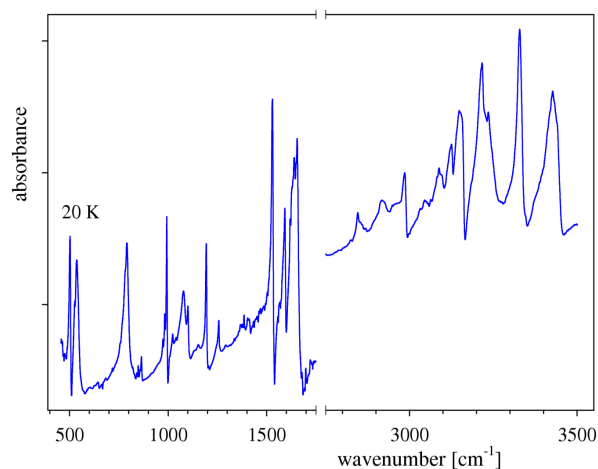
Fig. 3. FT-IR spectra of [4-apyH][SbCl$_4$] recorded in nujol at 20 K.

The structures of the [4-apyH]$^+$ cation and the [4-apyH][SbCl$_4$] complex were optimised by different quantum mechanical methods [10, 11, 13]. The structure of the isolated [4-apyH]$^+$ cation was optimised by the B3LYP/6-311G** method, while the structure of the complex — by the semi-empirical PM3 and B3LYP/LanL2Dz methods. The optimised structure of the complex obtained by the semi-empirical method is close to that determined by the X-ray studies [2]; the calculated angle N1–Cl–Sb is 91° while X-ray data give 93°. The bond length and internal angles of the skeleton of the optimised structures are collected in Table I. The data are also compared with the X-ray diffraction structure determined at 100 K [2].

The values of RMS^* were calculated in order to compare the structure of the [4-apyH]$^+$ cation optimised by different methods with the X-ray data, according to the formula

$$RMS = \sqrt{\frac{\sum (x_{\mathrm{cal}} - x_{\mathrm{exp}})^2}{n}},$$

where x_{cal} and x_{exp} are the calculated and experimental data, respectively. They are 0.008 Å and 0.16° for the bond length and internal angles, respectively. On the other hand, the RMS were also calculated to compare the bond lengths and angles of the [4-apyH][SbCl$_4$] complexes optimised by the B3LYP/LanL2Dz and PM3 methods with the experimental X-ray data; then the RMS values are: 0.074 Å, 2.06° and 0.112 Å, 6.86°, respectively. Therefore, the optimisation of the skeleton structure of the studied complex of [4-apyH][SbCl$_4$] by the DFT method gives a better approximation of its internal structure.

Then the frequencies and intensities of normal modes in the vibrational spectrum were calculated by quantum chemistry (QC) methods. Figure 4 shows a comparison of the low-temperature $G_{\mathrm{exp}}(\nu)$ spectrum and the calculated one.

TABLE I

Geometry of [4-apyH]$^+$ and [4-apyH][SbCl$_4$] complex.

| Bond	Bond length			
	[4-apyH][SbCl$_4$] [Å]			[4-apyH]$^+$ [Å]
	X-ray diffraction (100 K) [2]	B3LYP/ LanL2Dz	PM3	B3LYP/ 6-311G**
N1-C2	1.356	1.362	1.372	1.358
C2-C3	1.353	1.385	1.383	1.364
C3-C4	1.419	1.428	1.412	1.423
C4-C5	1.411	1.422	1.410	1.423
C5-C6	1.365	1.386	1.384	1.364
C6-N1	1.351	1.362	1.371	1.358
N2-C4	1.344	1.369	1.400	1.336
Sb1-Cl1	2.383	2.515	2.322	
Sb1-Cl2	2.683	2.815	2.336	
Sb1-Cl3	2.618	2.544	2.539	
Sb1-Cl4	2.378	2.512	2.342	
RMS		≈ 0.074	≈ 0.112	$RMS^* \approx 0.008$
Internal angles	Internal angles			
	[4-apyH][SbCl$_4$] [°]			[4-apyH]$^+$ [°]
	X-ray diffraction (100 K) [2]	B3LYP/ LanL2Dz	PM3	B3LYP/ 6-311G**
N1-C2-C3	120.75	120.64	121.08	120.61
C2-C3-C4	119.85	119.63	119.55	119.95
C3-C4-C5	117.72	117.93	118.67	117.44
C4-C5-C6	119.76	119.57	119.67	119.95
C5-C6-N1	120.57	120.67	120.96	120.61
C6-N1-C2	121.32	121.55	120.06	121.43
C3-C4-N2	121.07	121.05	120.54	121.28
C5-C4-N2	121.21	121.02	120.61	121.28
Cl1-Sb1-Cl2	88.77	86.02	100.80	
Cl1-Sb1-Cl3	89.73	92.56	101.42	
Cl1-Sb1-Cl4	92.57	96.73	94.25	
Cl2-Sb1-Cl3	173.93	172.76	157.26	
Cl2-Sb1-Cl4	86.70	85.90	93.24	
Cl3-Sb1-Cl4	87.49	82.54	80.34	
RMS		≈ 2.06	≈ 6.86	$RMS^* \approx 0.16$
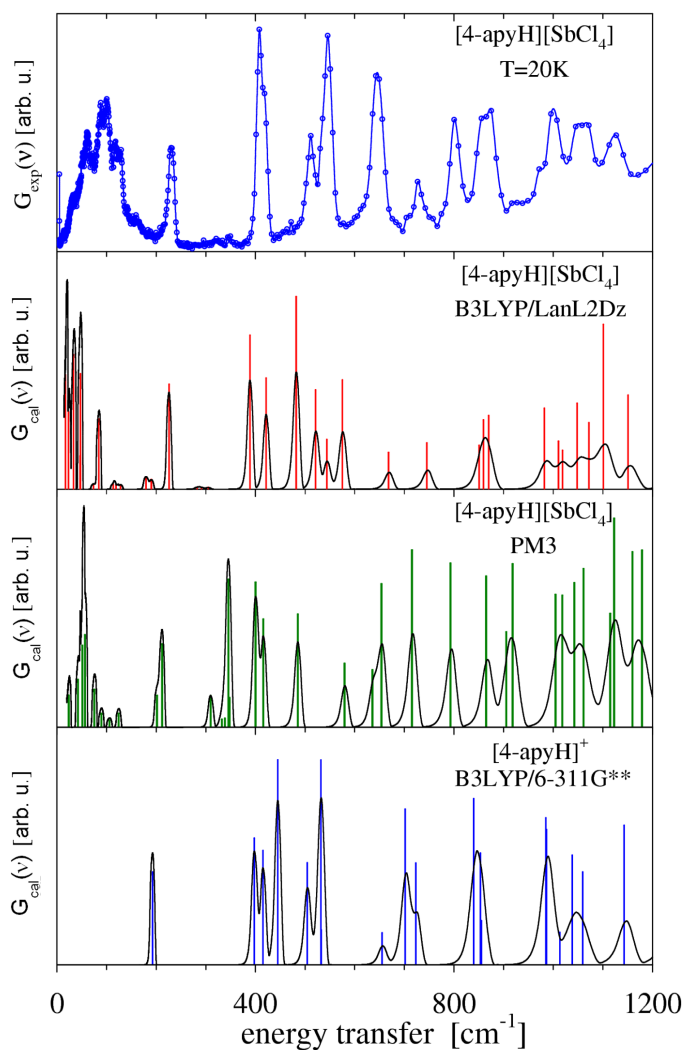
Fig. 4. The phonon density of state spectra of [4-apyH][SbCl$_4$] obtained at 20 K after transformation of the IINS spectra in one phonon scattering approximation $G_{\exp}(\nu)$. The $G_{\mathrm{cal}}(\nu)$ spectra of [4-apyH]$^+$ calculated by DFT method B3LYP/6-311G**. The $G_{\mathrm{cal}}(\nu)$ spectra of [4-apyH][SbCl$_4$] calculated by B3LYP/LanL2Dz and semi-empirical PM3 methods; each calculated band is convoluted with the resolving power of the NERA spectrometer.

Table II collects the frequencies of the bands obtained by the neutron $G_{\exp}(\nu)$ and FT-IR spectroscopy at 20 K, as well as the frequencies of normal modes calculated by the PM3 and B3LYP/LanL2Dz for the complex and also by B3LYP/6-311G* for the [4apy-H] cation (columns: A — Frequencies of IINS at

TABLE II

Comparison of the experimental and calculated frequencies of normal modes by different QC methods of [4-apyH][SbCl$_4$] complex.

A	D	E	Assignment and potential energy distribution (PED) [%]
	17.3	23.7	δ[Cl3-Sb1-Cl1] 35% δ[Cl3-Sb1-Cl2] 20% δ[Cl4-Sb1-Cl2] 14% δ[Cl1-Sb1-Cl2] 11% χ[N1-Cl3] 6%
	23.3	42.6	χ[Cl3-Sb1] 61% χ[N1-C2] 7% χ[N1-C6] 6% δ[Cl4-Sb1-Cl2] 5%
35.8	33.6	51.3	δ[C2-N1-Cl3] 29% δ[C6-N1-Cl3] 27% χ[Cl3-Sb1] 14% δ[N1-Cl3-Sb1] 5%
52.7	46.6	56.4	χ[N1-Cl3] 69% χ[N1-C2] 9% χ[N1-C6] 7%
60.8	47.3	75.5	δ[N1-Cl3-Sb1] 25% δ[Cl3-Sb1-Cl4] 19% δ[Cl4-Sb1-Cl2] 9% δ[C2-N1-Cl3] 7% δ[C6-N1-Cl3] 7%
70.9	73.7	89.6	δ[Cl1-Sb1-Cl2] 32% δ[Cl4-Sb1-Cl2] 22% δ[Cl3-Sb1-Cl1] 14% δ[N1-Cl3-Sb1] 9%
88.5	84.4	105.8	δ[Cl4-Sb1-Cl1] 88%
100.5	113.5	124.4	δ[Cl4-Sb1-Cl2] 63% δ[Cl3-Sb1-Cl4] 21%
117.5	119.1		

20 K [cm^{-1}], B — Wave numbers of IR at 20 K [cm^{-1}], C — Frequencies of [4-apyH]$^+$ by B3LYP/6-311G** [cm^{-1}], D — Frequencies of [4-apyH][SbCl$_4$] by B3LYP/LanL2Dz [cm^{-1}], E — Frequencies of [4-apyH][SbCl$_4$] by PM3 [cm^{-1}]). The assignment of the bands in the phonon density of state spectrum was predicted

TABLE II (cont.)

A	C	D	E	Assignment and PED [%]
129.6		128.0	201.6	ν[Cl3-Sb1] 56% ν[N1-Cl3] 10% δ[N1-Cl3-Sb1] 9%
160		179.4	211.9	χ[C3-C4] 31% χ[C4-C5] 31% ρ[C3-C4-N2] 11% ν[Cl3-Sb1] 6% ρ[C4-C5-C6] 6%
230.4	192.7	190.2	309.9	ν[N1-Cl3] 50% ν[Cl3-Sb1] 11% ν[Sb1-Cl4] 9% ν[Sb1-Cl2] 8%
320.9		225.9	332.5	ν[Sb1-Cl2] 83% ν[Cl3-Sb1] 9%
		282.7	338.4	ν[Sb1-Cl4] 80% ν[Sb1-Cl1] 11%
		291.1	345.5	χ[C4-N2] 58% χ[C2-C3] 13% χ[C6-C5] 12%
349.3		304.7	347.7	ν[Sb1-Cl1] 83% ν[Sb1-Cl4] 9%
407.8	397.7	389.2	400.2	χ[C2-C3] 32% χ[C6-C5] 31% χ[C4-N2] 10% χ[N1-C2] 8% χ[N1-C6] 5%
418.3	415.3	421.6	415.9	δ[C3-C4-N2] 34% δ[N2-C4-C5] 34% χ[C6-C5] 7% χ[C2-C3] 7%
471.5	445.1	482.2	485.2	ρ[C3-C4-N2] 48% χ[N1-C6] 18% χ[N1-C2] 17% χ[C6-C5] 6%

by the PM3 method. According to the results of the calculations, performed by the PM3 and B3LYP/6-311G** methods, the bands at the low neutron energy transfer (in the lattice branch) of the $G_{\exp}(\nu)$ spectrum can be interpreted as the

TABLE II (cont.)

A	B	C	D	E	Assignment and PED [%]
510.4	502	504.4	521.2	579.6	ν[N1-Cl3] 21% δ[C3-C4-C5] 20% ν[C4-N2] 13% δ[C2-C3-C4] 7% δ[C4-C5-C6] 7%
544.8	526	531.8 532.6	543.7	635.8	δ[N1-C6-C5] 20% δ[N1-C2-C3] 19% δ[C4-C5-C6] 18% δ[C2-C3-C4] 17%
			575.3	653.9	χ[C6-C5] 30% χ[C2-C3] 28% ρ[C3-C4-N2] 24%
642-648		665.2	668.2	715.5	δ[C4-N2-H] 16% δ[C4-N2-H] 13% ρ[C3-C4-N2] 11% δ[H-N2-H] 11% χ[N1-C2] 8%
725.9	725 768	701.6 723.1	745.6	793.1	δ[C4-N2-H] 16% δ[C4-N2-H] 16% ν[C4-N2] 12% δ[H-N2-H] 11% ρ[C4-C5-C6] 10%
800.5	792	839.8	850.9	864.8	ρ[C2-C3-C4] 31% ρ[N1-C2-C3] 25% χ[N1-C2] 13% ρ[C4-C5-C6] 12% χ[C3-C4] 7%
854.7	866	853.5 855.3	859.6	905.4	δ[C2-N1-C6] 14% δ[N1-C2-C3] 11% δ[N1-C6-C5] 11% ν[C4-N2] 10% ν[N1-Cl3] 7%
874.3			870.0	918.3	ρ[C4-C5-C6] 38% χ[N1-C6] 14% ρ[C3-C4-N2] 11% ρ[N1-C6-H] 9% ρ[C2-C3-C4] 8%

TABLE II (cont.)

A	B	C	D	E	Assignment and PED [%]
925.7 994.8	974 983 997	985.2 986.5	982.3	1004.7	χ[C2-C3] 29% ρ[C2-C3-C4] 28% ρ[N1-C2-C3] 25%
			1010.6	1018.3	ρ[N1-C6-H] 33% χ[C6-C5] 28% ρ[C4-C5-C6] 21% χ[N1-C6] 8%
		1013.3	1018.8	1042.5	δ[N1-C2-H] 18% δ[N1-C6-H] 11% ν[C3-C4] 10% δ[C3-C2-H] 8% δ[C4-C5-H] 7%
1059±10	1025	1038.4	1048.2	1061.0	δ[C4-N2-H] 36% δ[C4-N2-H] 35% ν[C4-C5] 8%
	1079	1059.6	1072.1	1114.7	ν[C4-N2] 12% δ[C3-C2-H] 10% ν[N1-C2] 9% ν[N1-C6] 8% δ[H-C6-C5] 6%
1126±10	1101		1101.0	1122.6	δ[H-C6-C5] 12% δ[N1-C6-H] 10% δ[C2-C3-H] 10% δ[C4-C3-H] 9% δ[C6-C5-H] 9%
1218±15		1143.1	1150.8	1159.5	δ[C6-C5-H] 21% δ[C4-C5-H] 20% δ[C2-C3-H] 13% δ[C4-C3-H] 12% δ[N1-C2-H] 11%

deformation in-plane, torsional out-of-plane, or stretching vibrations of the anion $[SbCl_4]^-$.

The band observed at 230.4 cm^{-1} can be interpreted according to the PM3 calculation results as the stretching vibrations ν [N1...Cl3], ν [Cl3–Sb1], ν [Sb1–Cl4], ν [Sb1–Cl2], but the first internal torsional out-of-plane mode of cation is given at 211.9 cm^{-1}. The calculations performed by

QC/B3LYP/LanL2Dz and B3LYP/6-311G** methods predict it at 190.2 and 192.7 cm^{-1}, respectively. However, a comparison of the vibrational spectrum calculated for the isolated cation of [4-apyH]$^+$ and the experimental neutron scattering ones permits concluding that the strong band at 230 cm^{-1} observed in the lattice branch is an internal mode of the cation.

The most intense band in the low-temperature phonon density of state spectrum $G_{\mathrm{exp}}(\nu)$ of [4-apyH][SbCl$_4$] appears at the energy transfer of 407.8 cm^{-1}. On the basis of the PM3 calculations the band at 400.2 cm^{-1} is assigned as the out-of-plane torsion of the 4-aminopyridinum cation: χ [C4–N2], χ [N1–C2], χ [N1–C6], χ [C2–C3], χ [C6–C5]. The DFT methods predict this band at 389.2 and 397.7 cm^{-1} for the complex, which is presented in Fig. 1, and for the isolated cation, respectively.

Another intense band is observed in the $G_{\mathrm{exp}}(\nu)$ spectrum at the energy transfer of 544.8 cm^{-1}. The PM3 calculations predict a band at 635.8 cm^{-1} which may be interpreted as the deformation in-plane: δ [N1–C6–C5], δ [N1–C2–C3], δ [C4–C5–C6], δ [C2–C3–C4]. According to this assignment, the intense $G_{\mathrm{exp}}(\nu)$ band in the low-temperature spectrum is related to the dynamics of the N(1)H$^+$ group and therefore its intensity should decrease on heating. The B3LYP/6-311G** calculations predict it at 531.8 and 532.6 cm^{-1}, while B3LYP/LanL2Dz — at 543.7 cm^{-1}. Intermolecular interactions of hydrogen bridge bond type between the donor –N$^+$H group and the acceptor take place in the crystal. They influence the internal structure of the cation; consequently, the frequencies of internal normal modes in the cation and in the complex are different.

The subsequent band appears at 645 cm^{-1}. The PM3 calculation gives the normal mode at 715.5 cm^{-1} which may be assigned as deformational in-plane δ [C4–N2–H], δ [H–N2–H], out-of-plane torsion vibration of the 4-aminopiridinium cation χ [N1–C2] and out-of-plane vibration ρ [C3–C4–N2]. According to the B3LYP/LanL2Dz and B3LYP/6-311G** calculations they are at 668.2 cm^{-1} and 665.2 cm^{-1}, respectively.

Another intense band is observed in the $G_{\mathrm{exp}}(\nu)$ spectrum at the energy transfer 800.5 cm^{-1}. On the basis of the PM3 calculations the band at 864.8 cm^{-1} is assigned as the out-of-plane vibration of the 4-aminopyridinum cation: ρ [C2–C3–C4], ρ [N1–C2–C3], ρ [C4–C5–C6] and the torsional out-of-plane χ [N1–C2], χ [C3–C4]. The calculations for the [4-apyH][SbCl$_4$] complex and for the isolated cation predict this band at 850.9 and 839.8 cm^{-1}, respectively.

The vibrational spectra calculated by QC methods also permit analysis of the normal modes in IR spectra. Figure 5 presents a comparison of the spectrum recorded experimentally at 20 K and that calculated by the B3LYP/LanL2Dz method. The frequencies of the observed normal modes (from neutron scattering as well as from IR data) and the unscaled calculated frequencies for 67 vibrational normal modes are plotted in Fig. 6. The slope of this dependence is 0.998. It may be noted that the deviations of the experimental frequencies from the calculated
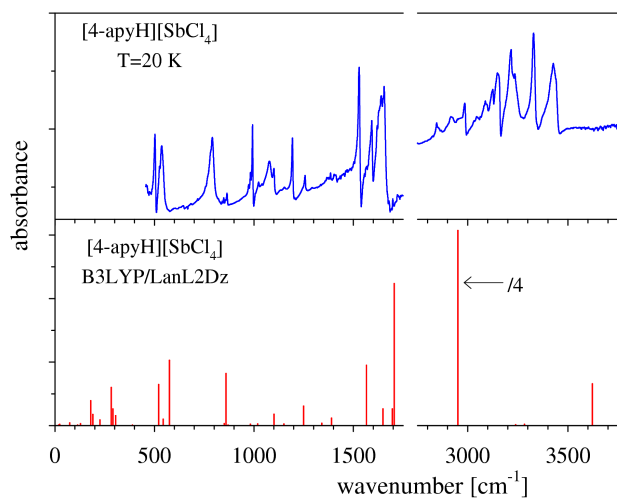
Fig. 5. Infrared absorbance of [4-apyH][SbCl$_4$] obtained at 20 K and bars calculated by QC method B3LYP/LanL2Dz.
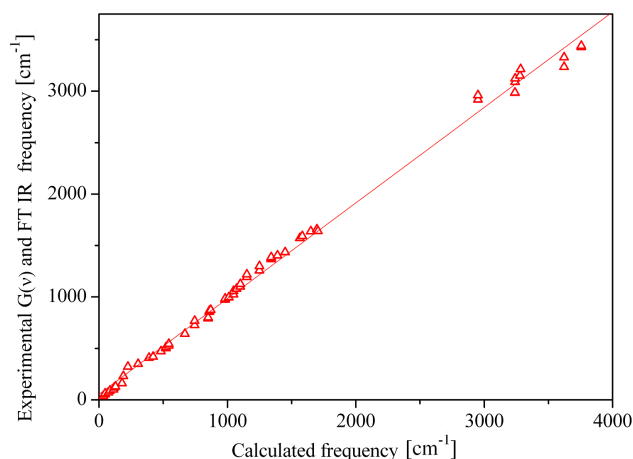

Fig. 6. Comparison of frequencies of normal modes obtained experimentally by neutron and IR methods (symbols). The lines were obtained after linear fit of both results.

ones are within several percents. The effect of vibrational anharmonicity seems to be negligible. The stretching modes are mainly red shifted, as shown in Figs. 5 and 6, because of the hydrogen bridge interaction. Also these stretching vibrations ν [N–H] at 2986, 3216, 3328, and 3429 cm^{-1} at 20 K undergo shifting on heating [15]. The observed changes in the intensity of $G_{\mathrm{exp}}(\nu)$ and the temperature shift of the IR bands at 502, 790, 1194, 2986, 3216, 3329 cm^{-1} [15] indicate an important role of the N–H—Cl interactions.

4. Summary

Using the *ab initio* and semi-empirical calculations the influence of the N1–H...Cl(3) hydrogen bridge interactions in [4-apyH][SbCl$_4$] on the vibrational spectra has been studied. According to the X-ray data, the bond is nearly linear, the characteristic N1–H...Cl angle is 172.39°, and its length is 3.267 Å [2]. The geometries of the complex, the strongest interaction in it and vibrational frequencies have been obtained. The semi-empirical calculations give the structure of the complex analysed close to that following from the X-ray diffraction study. The influence of the hydrogen bridge on the internal structure and the vibrational spectra ($G_{exp}(\nu)$ and FT-IR absorbance) has been determined. The observed decrease in the intensity of selected normal modes in the $G_{exp}(\nu)$ spectra on heating has been interpreted as corresponding to the increasing dynamics of protons.

Acknowledgments

References

[1] R. Jakubas, Z. Ciunik, G. Bator, *Phys. Rev. B* **67**, 024103 (2003).

[2] CCDC No. 185826–185828. Copies of this information may be obtained free of charge from the Director, CCDC, 12 UNION Road, Cambridge CB2 1EZ, UK (e-mail: deposit@ccdc.cam.ac.uk or http:////www.ccdc.cam.ac.uk).

[3] F.H. Allen, *Acta Crystallogr. B* **58**, 380 (2002).

[4] I.J. Bruno, J.C. Cole, P.R. Edgington, M. Kessler, C.F. Macrae, P. McCabe, J. Pearson, R. Taylor, *Acta Crystallogr. B* **58**, 389 (2002).

[5] C.F. Macrae, P.R. Edgington, P. McCabe, E. Pidcock, G.P. Shields, R. Taylor, M. Towler, J. van de Streek, *J. Appl. Crystallogr.* **39**, 453 (2006).

[6] I.J. Bruno, J. Cole, J.P.M. Lommerse, R.S. Rowland, R. Taylor, M. Verdonk, *J. Comput. Aid. Mol. Des.* **11**, 525 (1997).

[7] I.J. Bruno, J.C. Cole, M. Kessler, J. Luo, W.D.S. Motherwell, L.H. Purkis, B.R. Smith, R. Taylor, R.I. Cooper, S.E. Harris, A.G. Orpen, *J. Chem. Inf. Comp. Sci.* **44**, 2133 (2004).

[8] M.L. Verdonk, J.C. Cole, R. Taylor, *J. Mol. Biol.* **289**, 1093 (1999).

[9] *Neutron Data Booklet*, Eds. A.J. Dianoux, G. Lander, ILL Neutrons for Sciences, Grenoble 2003.

[10] A.D. Becke, *J. Chem. Phys.* **97**, 9173 (1992); *J. Chem. Phys.* **98**, 5648 (1993); C. Lee, W. Yang, R.G. Parr, *Phys. Rev. B* **37**, 785 (1988).

[11] I.J.P. Stewart, *J. Mol. Model.* **10**, 155 (2004); *J. Comp. Chem.* **12**, 320 (1991), *ibid.* **10**, 209 (1989); **10**, 221 (1989); V.D. Khavryutchenko, *COSPECO Complex Program for Vibrational Spectroscopy*, Institute of Surface Chemistry, Ukrainian Academy of Sciences, Kiev 1990.

[12] I. Natkaniec, S.I. Bragin, J. Brankowski, J. Mayer, in *Proc. ICANS XII Meeting, Abington 1993*, Vol. I, 1994, RAL Report, 94-025, I, p. 89.

[13] M.J. Frish, G.W. Trucks, H.B. Schlegel, G.E. Scuseria, M.A. Robb, J.R. Cheeseman, V.G. Zakrzewski, J.A. Montgomery, R.E. Stratmann, J.C. Burant, S. Dapprich, J.M. Millam, A.D. Daniels, K.N. Kudin, M.C. Strain, O. Farkas, J. Tomasi, V. Barone, M. Cossi, R. Cammi, B. Mennucci, C. Pomeli, C. Adamo, S. Clifford, J. Ochterski, G.A. Patersson, P.Y. Ayala, Q. Cui, K. Morokuma, D.K. Malick, A.D. Rabuck, K. Raghavachari, J.B. Foresman, J. Cioslowski, J.V. Ortiz, B.B. Stefanov, G. Liu, A. Liashenko, P. Piskorz, I. Komaromi, R. Gomperts, R.L. Martin, D.J. Fox, T. Keith, M.A. Al-laham, C.Y. Peng, A. Nanayakkara, C. Gonzalez, M. Challacombe, P.M.W. Gill, B.G. Johnson, W. Chen, M.W. Wong, J.L. Andres, M. Head-Gordon, E.S. Replogle, J.A. Pople, *GAUSSIAN 03*, Gaussian, Inc., Pittsburgh PA, 2003.

[14] W.J. Kazimirov, I. Natkaniec, Preprint P14-2003-48 JINR, Dubna 2003.

[15] K. Holderna-Natkaniec, I. Natkaniec, J. Swiergiel, unpublished results; J. Swiergiel, Ph.D. Thesis, IF UAM, Poznań 2007.